

Suppression of the multi-azimuthal-angle instability in dense neutrino gas during supernova accretion phase

Sovan Chakraborty,¹ Alessandro Mirizzi,² Ninetta Saviano,³ and David de Sousa Seixas¹

¹*Max-Planck-Institut für Physik (Werner-Heisenberg-Institut)
Föhringer Ring 6, D-80805 München, Germany*

²*II Institut für Theoretische Physik, Universität Hamburg,
Luruper Chaussee 149, 22761 Hamburg, Germany*

³*Institute for Particle Physics Phenomenology, Department of Physics, Durham University,
Durham DH1 3LE, United Kingdom*

It has been recently pointed out that removing the axial symmetry in the “multi-angle effects” associated with the neutrino-neutrino interactions for supernova (SN) neutrinos, a new multi-azimuthal-angle (MAA) instability would arise. In particular, for a flux ordering $F_{\nu_e} > F_{\bar{\nu}_e} > F_{\nu_x}$, as expected during the SN accretion phase, this instability occurs in the normal neutrino mass hierarchy. However, during this phase the ordinary matter density can be larger than the neutrino one, suppressing the self-induced conversions. At this regard, we investigate the matter suppression of the MAA effects, performing a linearized stability analysis of the neutrino equations of motion, in the presence of realistic SN density profiles. We compare these results with the numerical solution of the SN neutrino non-linear evolution equations. Assuming axially symmetric distributions of neutrino momenta we find that the large matter term strongly inhibits the MAA effects. In particular, the hindrance becomes stronger including realistic forward-peaked neutrino angular distributions. As a result, in our model for a $10.8 M_\odot$ iron-core SNe, MAA instability does not trigger any flavor conversion during the accretion phase. Instead, for a $8.8 M_\odot$ O-Ne-Mg core SN model, with lower matter density profile and less forward-peaked angular distributions, flavor conversions are possible also at early times.

PACS numbers: 14.60.Pq, 97.60.Bw

I. INTRODUCTION

The flavor evolution of supernova (SN) neutrinos, is strongly impacted by the self-induced effects, associated with instabilities induced by the the neutrino-neutrino interactions in the deepest stellar regions [1–8] (see also [9] for a recent review). In this context a key ingredient in the characterization of these effects is related to the current-current nature of low-energy weak interactions, which implies a “multi-angle term” [5, 10] $(1 - \mathbf{v}_\mathbf{p} \cdot \mathbf{v}_\mathbf{q})$, where $\mathbf{v}_\mathbf{p}$ is the neutrino velocity [2]. Till recently, all studies have assumed the axial symmetry for this term, that would then depend only on the zenith-angle. It has been shown that the “multi-zenith-angle” (MZA) term in some cases can hinder the maintenance of the coherent oscillation behavior for different neutrino modes [5, 7, 10–13].

A valuable tool to diagnose the possible instabilities of a dense neutrino gas is given by the linearized stability analysis of the neutrino equations of motion. The linearized equations including generic azimuthal and zenith angle distributions for neutrinos were first worked out in [10]. Then, the formalism for the azimuthal symmetric case was further developed in [14]. The stability method would allow one to determine the possible onset of the flavor conversions, seeking for an exponentially growing solution of the eigenvalue problem, associated with the linearized equations of motion for the neutrino ensemble. Recently, this method has been applied in [15] removing the assumption of axial symmetry

in the ν propagation. As a result, a multi-azimuthal-angle (MAA) instability was found in addition to the bimodal [16] and MZA ones [15]. In particular, it was considered a neutrino ensemble with a strong excess of ν_e over $\bar{\nu}_e$, as expected during the SN accretion phase (at post-bounce times $t_{\text{pb}} \lesssim 0.5$ s). In this situation, the instability has been found in normal mass hierarchy (NH, $\Delta m_{\text{atm}}^2 = m_3^2 - m_{1,2}^2 > 0$), where the system would have been stable imposing the perfect axial symmetry. Subsequently, the role of this instability has been clarified in [17, 18] with simple toy models. The discovery of the new MAA effects, has also motivated first numerical studies of the non-linear neutrino propagation equations in SN, introducing the azimuthal angle as angular variable in the multi-angle kernel, in addition to the usual zenith angle [19, 20]. Remarkably it was considered the ν propagation only along a radial direction, i.e. a local solution along a specific line of sight, under the assumption that the transverse variations of the global solution are small. In this approximation, for the unstable case discussed above, MAA effects lead in NH to spectral swaps and splits analogous to what produced in inverted hierarchy (IH, $\Delta m_{\text{atm}}^2 < 0$) by the known bimodal instability [16] also in a completely isotropic neutrino gas [21].

All these recent works assume that the MAA effects can develop without any matter hindrance. Remarkably, a crucial ingredient to be considered to determine the impact of self-induced flavor instabilities is the ordinary matter term, associated with the net electron densities n_e in SNe. As pointed out in [22] for the axial-symmetric

case, when n_e is not negligible with respect to the neutrino density n_ν , the large phase dispersion induced by the matter for ν 's traveling in different directions, would partially or totally suppress the self-induced oscillations through peculiar MZA effects. Recent studies of this case performed with realistic SN models, indicates that this situation is realized during the supernova accretion phase (at post-bounce times $t_{\text{pb}} \lesssim 0.5$ s). As a consequence, the self-induced flavor conversions found in IH in the axial-symmetric models are strongly inhibited [23–26].

From a preliminary schematic study done in [15] it results that the matter density required to suppress the MMA instability in NH is larger than the one necessary to suppress the self-induced conversions in IH for the axial symmetric case. Motivated by these previous results, we find it is mandatory to understand what is the role of the dense matter on the MAA effects during the accretion phase. We will use as benchmark for the neutrino and matter density profiles the SN models from recent long term simulations of core-collapse explosions, performed by the Basel-Darmstadt model. These were already considered by some of us in [23–25]. The plan of our work is as follows. In Sec. 2 we present the neutrino equations of flavor evolution without imposing axial asymmetry. Then, we describe the setup to perform the stability analysis of the linearized equations of motion. In Sec. 3 we present the results of the stability analysis and we compare them with the numerical solution of the equations. We focus on the accretion phase for two different SN progenitor models. Finally, in Sec. 4 we comment on our results and we conclude.

II. SETUP OF THE FLAVOR EVOLUTION

A. Equations of flavor evolution

In the axial symmetric case, the SN neutrino flavor evolution is described by ordinary differential equations [27], characterizing the flavor changes along a radial direction. When axial symmetry is broken by the MAA effects, in order to get the global solution of the problem in general one would consider also variations along the transverse direction to the neutrino propagation. This would imply passing from ordinary to partial differential equations, with a big layer of complication in the numerical solution. However, in our study we are mostly interested in answering the question of the stability of the dense neutrino gas under MMA effects, in the presence of a large matter term. Therefore, *before* the MAA instability emerges, we can still consider the ordinary differential equations in the only radial direction. These are enough to determine which cases are completely stable under MAA effects. In the other cases, in which the MAA instability develops, these equations would be useful to determine the onset radius of the flavor conversions. Nevertheless, the subsequent flavor evolution can be taken just as indicative, since it is based on the assumption that variations in the

transverse direction always remain small.

Under this approximation, the flavor evolution depends only on r , E and \mathbf{v}_p . Then, following [14, 15] we write the equations of motion for the flux matrices $\Phi_{E,u,\varphi}$ as function of the radial coordinate. We use negative energy E for anti-neutrinos. Following the usual prescription, we label the zenith angular mode in terms of the variable $u = \sin^2 \theta_R$, where θ_R is the emission angle relative to the radial direction of the neutrinosphere radius R_ν [12, 14]. We call φ the azimuth angle of the neutrino velocity \mathbf{v}_p . We normalize the flux matrices to the $\bar{\nu}$ number flux at the neutrinosphere. The diagonal $\Phi_{E,u,\varphi}$ elements are the ordinary number fluxes integrated over a sphere of radius r . The off-diagonal elements, which are initially zero, carry a phase information due to flavor mixing. Then, the equations of motion read [14, 15]

$$i\partial_r \Phi_{E,u,\varphi} = [H_{E,u,\varphi}, \Phi_{E,u,\varphi}] , \quad (1)$$

with the Hamiltonian [15]

$$H_{E,u} = \frac{1}{v_u} \left(\frac{M^2}{2E} + \sqrt{2} G_F N_l \right) + \frac{\sqrt{2} G_F}{4\pi r^2} \int d\Gamma'_{E,u,\varphi} \left(\frac{1 - v_u v_{u'} - \boldsymbol{\beta} \cdot \boldsymbol{\beta}'}{v_u v_{u'}} \right) \Phi' . \quad (2)$$

The matrix M^2 of neutrino mass-squares causes vacuum flavor oscillations. We work in a two-flavor scenario, associated with the atmospheric mass-square difference $\Delta m_{\text{atm}}^2 = 2 \times 10^{-3} \text{ eV}^2$ and a small (matter suppressed) in-medium mixing $\Theta = 10^{-3}$. We will always consider NH, where MAA effect could emerge for the flux ordering we are considering. The matrix $N_l = \text{diag}(n_e, 0, 0)$ in flavor basis, contains the net electron density and is responsible for the Mikheyev-Smirnov-Wolfenstein (MSW) matter effect [28] with the ordinary background. Finally, the term at second line represents the ν - ν refractive term, where $\int d\Gamma_{E,u,\varphi} = \int_{-\infty}^{+\infty} dE \int_0^1 du \int_0^{2\pi} d\varphi$. In the multi-angle term of Eq. (2), the radial velocity of a mode with angular label u is $v_u = (1 - u R_\nu^2 / r^2)^{1/2}$ [12] and the transverse velocity is $\beta_u = u^{1/2} R_\nu / r$ [15]. The term $\boldsymbol{\beta} \cdot \boldsymbol{\beta}' = \sqrt{uu'} R_\nu^2 / r^2 \cos(\varphi - \varphi')$ is the responsible for the breaking of the axial symmetry.

To solve numerically Eq. (1) we use an integration routine for stiff ordinary differential equations taken from the NAG libraries [29] and based on an adaptive method. We have used $N_\varphi = 30$ modes for $\varphi \in [0; 2\pi]$, $N_u = 1400$ for $u \in [0; 1]$. Concerning neutrino emission model, in order to simplify the complexity of our numerical simulations of the flavor evolution, we assume all ν 's to be represented by a single energy, that we fix at $E = 15 \text{ MeV}$. This approximation is reasonable since our main purpose is to determine only if the dense matter effects block the development of the self-induced transformations.

B. Stability conditions

In order to perform the stability analysis, we linearize the equations of motion [Eq. (2)], following the approach of [14, 15]. We write the flux matrices in the form

$$\Phi_{\omega,u} = \frac{\text{Tr}\Phi_{\omega,u,\varphi}}{2} + \frac{g_{\omega,u,\varphi}}{2} \begin{pmatrix} s & S \\ S^* & -s \end{pmatrix}, \quad (3)$$

where we switch to the frequency variable $\omega = \Delta m_{\text{atm}}^2/2E$, and we introduce the neutrino flux difference distributions $g_{\omega,u,\varphi} \equiv g(\omega, u, \varphi)$ that represent the flavor fluxes $n_{\nu_e}(R_\nu) - n_{\nu_x}(R_\nu)$ at the neutrinosphere, normalized to the $\bar{\nu}$ flux. In the following we will always assume axial symmetry of the neutrino emission. Therefore $g(\omega, u, \varphi) = g(\omega, u)/2\pi$. The $\text{Tr}\Phi_{\omega,u,\varphi}$ is conserved and then irrelevant for the flavor conversions. The ν_e survival probability is $\frac{1}{2}(1+s)$, given in terms of the swap factor $-1 \leq s \leq 1$ of the matrix in the second term on the right-hand side. The off-diagonal components S are complex and $s^2 + |S|^2 = 1$. The initial conditions are $s = 1$ and $S = 0$. Self-induced flavor transitions start when the off-diagonal term S grows exponentially.

In the small-amplitude limit $|S| \ll 1$, and at far distances from the neutrinosphere $r \gg R_\nu$, the linearized evolution equations for S assume the form [15]

$$i\partial_r S = [\omega + u(\lambda + \epsilon\mu)]S - \mu \int d\Gamma' [u + u' - 2\sqrt{uu'} \cos(\varphi - \varphi')] g' S' \quad (4)$$

In this equation $\epsilon = \int d\Gamma_{\omega,u,\varphi} g_{\omega,u,\varphi}$, quantifies the ‘‘asymmetry’’ of the neutrino spectrum, normalized to the $\bar{\nu}$ number flux. In the SN models we are using, typically $\epsilon \sim 0.3 - 0.5$ during the accretion phase (see Fig. 3 in [24]).

The ν - ν interaction strength is given by

$$\begin{aligned} \mu &= \frac{\sqrt{2}G_F [n_{\bar{\nu}_e}(R_\nu) - n_{\bar{\nu}_x}(R_\nu)] R_\nu^2}{4\pi r^2} \frac{R_\nu^2}{2r^2} \\ &= \frac{3.5 \times 10^9}{r^4} \left(\frac{L_{\bar{\nu}_e}}{\langle E_{\bar{\nu}_e} \rangle} - \frac{L_{\bar{\nu}_x}}{\langle E_{\bar{\nu}_x} \rangle} \right) \\ &\times \left(\frac{15 \text{ MeV}}{10^{52} \text{ erg/s}} \right) \left(\frac{R_\nu}{10 \text{ km}} \right)^2, \end{aligned} \quad (5)$$

while ordinary matter background term is given by

$$\begin{aligned} \lambda &= \sqrt{2}G_F n_e \frac{R_\nu^2}{2r^2} \\ &= \frac{0.95 \times 10^8}{r^2} \left(\frac{Y_e}{0.5} \right) \left(\frac{\rho}{10^{10} \text{ g/cm}^3} \right) \left(\frac{R_\nu}{10 \text{ km}} \right)^2 \end{aligned} \quad (6)$$

where Y_e is the net electron fraction, and ρ is the matter density. The radial distance r is expressed in km, while the numerical values of μ and λ in the two previous equations are quoted in km^{-1} , as appropriate for the SN case.

One can write the solution of the linear differential equation [Eq. (4)] in the form $S = Q_{\omega,u,\varphi} e^{-i\Omega r}$ with complex frequency $\Omega = \gamma + i\kappa$ and eigenvector $Q_{\omega,u,\varphi}$. A solution with $\kappa > 0$ would indicate an exponential increase in S , i.e. an instability. The solution of Eq. (4) can then be recast in the form of an eigenvalue equation for $Q_{\omega,u,\varphi}$. One gets as consistency condition [15]

$$\mu \int d\omega du \frac{u g_{\omega,u}}{\omega + u(\lambda + \epsilon\mu) - \Omega} + 1 = 0. \quad (7)$$

A flavor instability is present whenever Eq. (7) admits a solution (γ, κ) .

III. APPLICATION TO OUR SUPERNOVA MODELS

We consider the core-collapse supernova simulations of massive stars with 8.8 and 10.8 M_\odot progenitor from Ref. [30], taken as benchmark for our numerical study in [23–25]. The first type of SN belongs to the class of O-Ne-Mg-core progenitor. The second one is an iron-core progenitor.

Under the single-energy approximation we are using, we characterize the neutrino energy spectra as

$$\begin{aligned} g(\omega, u) &= \frac{1}{n_{\bar{\nu}_e} - n_{\bar{\nu}_x}} [(n_{\nu_e} g_{\nu_e}(u) - n_{\nu_x} g_{\nu_x}(u)) \delta(\omega - \omega_0) \\ &- (n_{\bar{\nu}_e} g_{\bar{\nu}_e}(u) - n_{\bar{\nu}_x} g_{\bar{\nu}_x}(u)) \delta(\omega + \omega_0)], \end{aligned} \quad (8)$$

where n_{ν_α} are the total number fluxes of the species ν_α at the neutrinosphere. In order to fix the neutrinosphere radius $r = R_\nu$, consistently with our choice in [23–25] we take the radius at which the ν_e 's angular distribution has no longer significant backward flux, i.e. a few % of the total one. This typically is in the range $R \sim 50 - 100$ km (see Fig. 4 in [24]).

For our choice of neutrino representative energy ($E = 15$ MeV), the corresponding frequency is

$$\omega_0 = \left\langle \frac{\Delta m_{\text{atm}}^2}{2E} \right\rangle = 0.34 \text{ km}^{-1}. \quad (9)$$

The $g_{\nu_\alpha}(u)$ represent the zenith-angle distributions. In our study we assume two different models. At first, we consider the ‘‘half-isotropic’’ case, where in analogy with a black-body emission, it is assumed $g_{\nu_\alpha}(u) = 1$ for all the species. We will then compare the results obtained in this widely used prescription, with the one obtained taking the $g_{\nu_\alpha}(u)$ directly from the output of the SN simulations. In this case, the zenith-angle distributions would be flavor-dependent and forward enhanced (i.e. peaked at small u) with respect to the half-isotropic emission model (see Fig. 1 and the discussion in [25]). We will see that the presence of forward peaked distributions will enhance the matter suppression of the MAA instability. Finally, we comment that our results are based on axial symmetric neutrino angular distributions. In this regard,

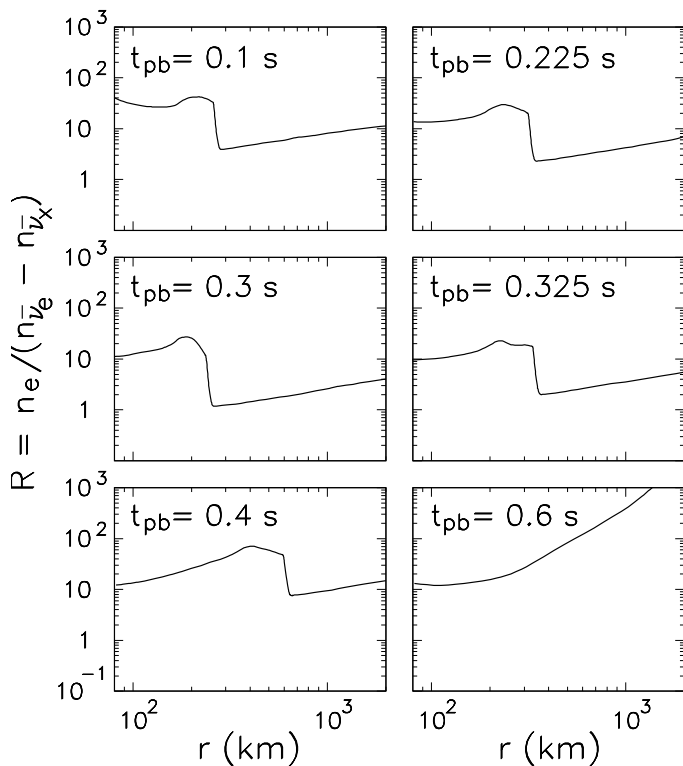


FIG. 1: $10.8 M_{\odot}$ progenitor mass. Radial evolution of the ratio R between the matter λ and neutrino μ potentials at different post-bounce times.

it is interesting to mention that in [10] it has been shown that if perfect cylindrical symmetry in the initial neutrino distributions were given up, super-fast flavor turnovers could be produced. We leave the investigation of this interesting issue for a future work.

A. $10.8 M_{\odot}$

We start our investigation with the case of the $10.8 M_{\odot}$ iron-core supernova. For this model, the net electron density n_e and the neutrino densities n_{ν} for different post-bounce times were shown in Fig. 5 of Ref. [24]. In order to quantify the relative strength of the matter potential λ [Eq. (6)] with respect to the neutrino potential μ [Eq. (5)] we plot in Fig. 1 the ratio $R = \lambda/\mu$ as a function of the radial coordinate r at different post-bounce times t_{pb} in the range $[0.1, 0.6]$ s. We realize that $R > 10$ before the abrupt discontinuity associated with the shock front position. As we will see with the stability analysis, this strong matter dominance would prevent the flavor conversions before the shock front. However, for some time snapshots (i.e. $t_{\text{pb}} = 0.225 - 325$ s) the ratio can become $R \gtrsim 1 - 2$ after the shock front, leaving the possibility of flavor conversions in this region.

For the same post-bounce times of Fig. 1, we show in

Fig. 2 the radial evolution of the eigenvalue κ determined from the solution of Eq. (7). We consider the following cases: (a) $\lambda = 0$ and a half-isotropic neutrino emission (dashed curves), (b) dense matter effects and a half-isotropic neutrino emission (continuous curves) and, (c) dense matter effects and non-trivial neutrino angular distributions (dotted curves). In Fig. 3 we show the survival probability P_{ee} for electron antineutrinos $\bar{\nu}_e$ for the same cases of Fig. 2, obtained solving the non-linear propagation equations [Eq. (2)].

We start discussing our results for the case of $\lambda = 0$ [case (a)]. We realize that when the neutrino system enters the unstable regime ($\kappa > 0$), the κ function rapidly grows from zero to a peak value greater than one. Only for $t_{\text{pb}} = 0.6$ s $\kappa \sim 0.3$ at the peak. Indeed, for this time the asymmetry parameter $\epsilon > 2$ (see Fig. 3 in [24]). Then the consistency condition Eq. (7) in order to be satisfied requires a smaller κ . Comparing the results of Fig. 2 and 3 one finds a good agreement between the numerical onset of the self-induced flavor conversions triggered by the MAA effect and the position of the peak in the κ function.

We now discuss the situation of realistic matter density profiles and a half-isotropic neutrino emission [case (b)]. As expected, the flavor instability is strongly suppressed with respect to the previous case without matter. In particular, the κ function, when not completely vanishing (as at $t_{\text{pb}} = 0.4$ s), would start growing only after the shock front position [see Fig. 1]. This is due to the fact that at lower radii the ratio $R \gg 1$. The κ function then reaches peak values between 0.5 and 1 only at intermediate times, i.e. $t_{\text{pb}} = 0.3, 0.325$ s, for which the ratio $R \gtrsim 1$ in the post-shock region. For the other time snapshots κ it is more suppressed, consistently with a larger value of R . Comparing these results with the numerical calculation of the P_{ee} in Fig. 3, we realize that the presence of a non-zero κ is not enough to guarantee the onset of flavor conversions. Indeed, for $t = 0.1, 0.6$ s, the κ function is too small and dies out too quickly before triggering flavor conversions. For the cases in which flavor conversions occur, i.e. at $t_{\text{pb}} = 0.225, 0.3, 0.325$ s, the numerical onset is shifted at larger radii by few hundred km, with respect to the peak of the κ function. This delay is due to the fact that since the instability is weaker with respect to the case with $\lambda = 0$, the slower rate of growth implies a larger radial distance in order to develop significant effects on the P_{ee} . We checked that a non-zero κ corresponds to the exponential growth of the off-diagonal components $S \sim e^{\kappa r}$ of the flux matrices [see Eq. (3)], while the change of the diagonal components, would occur only at larger radii. It would be interesting to see if the stability analysis can be further developed in order to achieve a better understanding of this dynamics.

Then we consider the case in which also the flavor-dependent forward-peaked neutrino angular distributions are taken into account [case (c)]. We find that the κ function in this case is completely suppressed. This is consistent with the expectation that the ν - ν strength is

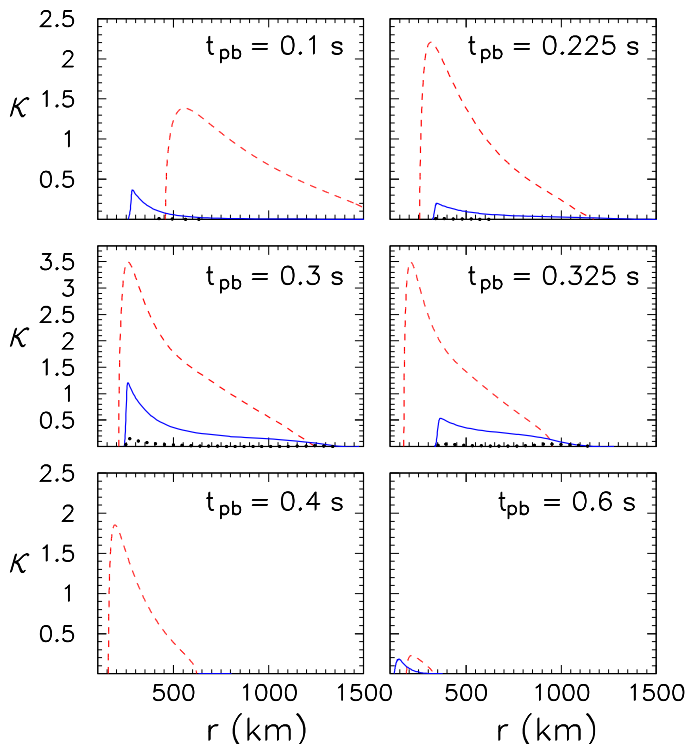


FIG. 2: $10.8 M_{\odot}$ progenitor mass. Radial evolution of the κ function (in units of km^{-1}) at different post-bounce times with $\lambda = 0$ for a half-isotropic neutrino emission (dashed curves) and in presence of matter effects, with a half-isotropic neutrino emission (continuous curves) and with flavor-dependent angular distributions (dotted curves).

weaker for forward-peaked distributions, making more effective the matter suppression. This result is consistent with the output of the numerical simulations that show for all the considered time snapshots $P_{ee} = 1$.

Finally we mention that in [31, 32] it has been claimed that possible residual scatterings could affect ν 's after the neutrinosphere, producing a small “neutrino halo” that would broaden the ν angular distributions [31, 32] at $r \gtrsim 100$ km. We checked that the results of the SN simulations we are using have not enough angular resolution to exhibit this feature. However, in order to characterize the possible halo effect, we performed the same analytical estimation presented in [32]. We repeated the stability analysis including the halo effect in the ν angular distributions, without finding any change with respect to the results shown here. Therefore, we conclude that for our $10.8 M_{\odot}$ SN model, MAA instability is always suppressed by the dense matter effects during the accretion phase.

B. $8.8 M_{\odot}$

In this section we analyze the flavor conversions for the model of $8.8 M_{\odot}$ O-Ne-Mg progenitor. In Fig. 4 we plot

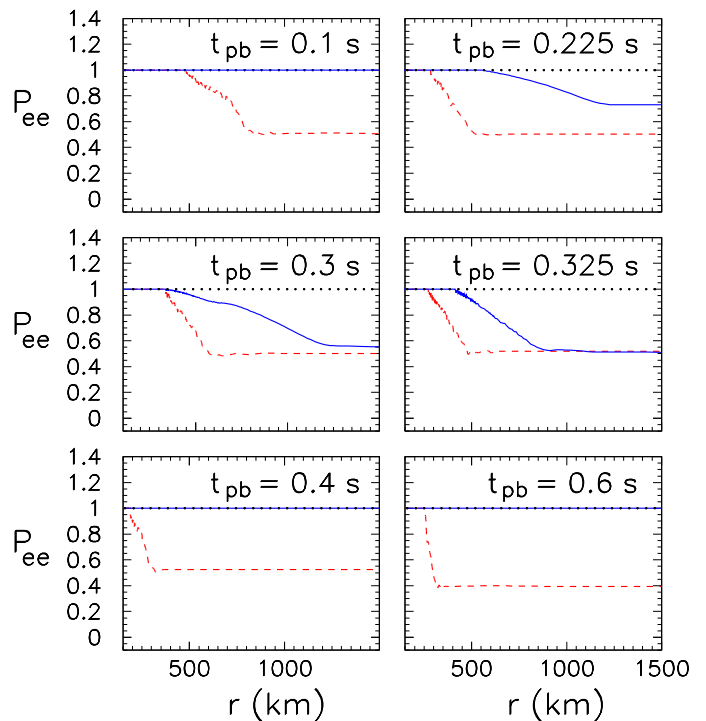


FIG. 3: $10.8 M_{\odot}$ progenitor mass. Radial evolution of the survival probability P_{ee} for electron antineutrinos at different post-bounce times for the MAA evolution with $\lambda = 0$ for a half-isotropic neutrino emission (dashed curves) and in presence of matter effects, with a half-isotropic neutrino emission (continuous curves) and with flavor-dependent angular distributions (dotted curves).

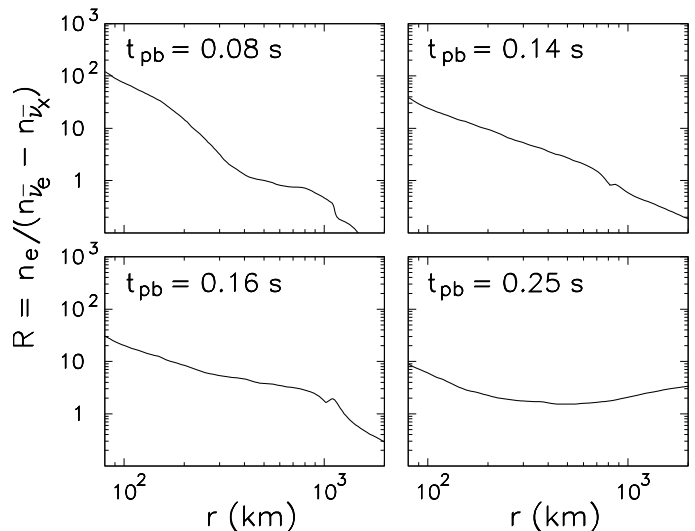


FIG. 4: $8.8 M_{\odot}$ progenitor mass. Radial evolution of the ratio R between the matter λ and neutrino μ potentials at different post-bounce times.

the ratio $R = \lambda/\mu$ for the same time snapshots of Fig. 9

of [24], i.e. in the range $[0.08, 0.25]$ s. We realize that in this case there is no abrupt discontinuity associated with the shock front. Indeed, for this low-mass progenitor there is no extended accretion phase, since the explosion succeeds very shortly after the core-bounce. Therefore, the shock-front is already beyond the radial range interesting for the flavor conversions. Since in this case the matter density of the envelope is low compared to the iron-core progenitors, the electron density profile above the core is very steep. Therefore, at $r \gtrsim$ few hundred km, the ratio $R \lesssim 3$ [for $t_{\text{pb}} \in [0.08, 0.16]$ s it monotonically decreases becoming also smaller than 1] suggests that flavor conversions could arise there.

In Fig. 5 we show the radial evolution of the eigenvalue κ for the time snapshots shown in Fig. 4, determined from the solution of Eq. (7). We use the same format of Fig. 2. In Fig. 6 we show the corresponding survival probability P_{ee} for electron antineutrinos $\bar{\nu}_e$. Starting with the case without matter term, i.e. $\lambda = 0$ (dashed curves), we see that the κ function rapidly becomes larger than 1, and the peak corresponds to the onset of the flavor conversions in Fig. 6. We pass now considering the case with λ and half-isotropic neutrino angular distributions (continuous curves). We realize that, for $t_{\text{pb}} = 0.08, 0.25$ s in the region where κ grows, $R \simeq 1 - 2$. Therefore, the matter suppression of the instability is never complete. Moreover, the rise of κ is rapid and the position of the peak corresponds to the onset of the flavor conversions seen in Fig. 6. Conversely, for the other time snapshots ($t_{\text{pb}} = 0.14, 0.16$ s) where $R \gtrsim 3$, the suppression of the instability is stronger. Moreover, the κ curves are broadened and there is not a clear peak. Therefore, one cannot easily link a non-zero κ with the numerical onset of the flavor conversions. In the case of λ and flavor dependent forward-peaked neutrino angular distributions (dotted curves), as expected we find a stronger suppression in the flavor instability. However, as shown in Fig. 1 of [25], the angular spectra of different flavors for the $8.8 M_{\odot}$ SN are significantly less forward-peaked than in the case of the $10.8 M_{\odot}$ SN. Therefore, their effect is less pronounced in this case. In particular, for $t_{\text{pb}} = 0.8, 0.25$ s, κ is large enough to trigger flavor conversions. Conversely, these are strongly inhibited at $t_{\text{pb}} = 0.14$ s, and completely suppressed for $t_{\text{pb}} = 0.16$ s.

Finally, we checked also in this case that including a possible halo effect does not change the results of the stability analysis. In conclusion, for our SN model with $8.8 M_{\odot}$ progenitor mass the matter suppression of the MAA instability is not complete at early times. Therefore, in principle one would expect interesting time-dependent features in the observable neutrino spectra.

IV. CONCLUSIONS

We have performed a dedicated study of the matter suppression of the MAA instability, connected with the axial symmetry breaking in the self-induced oscillations,

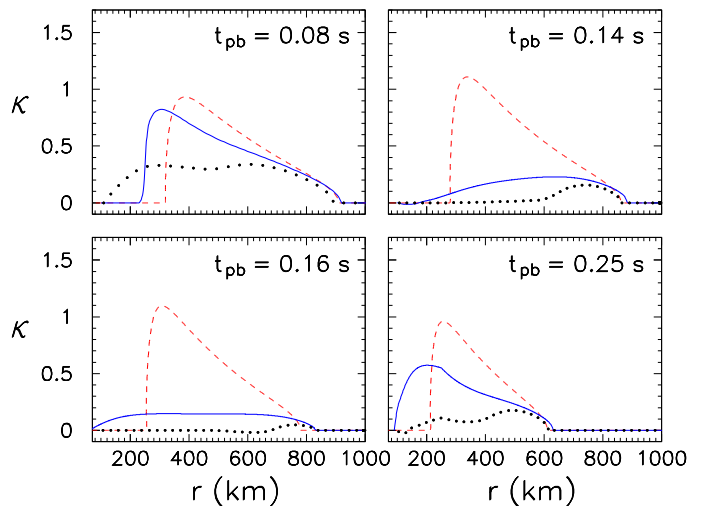


FIG. 5: $8.8 M_{\odot}$ progenitor mass. Radial evolution of the κ function (in units of km^{-1}) at different post-bounce times with $\lambda = 0$ for a half-isotropic neutrino emission (dashed curves) and in presence of matter effects, with a half-isotropic neutrino emission (continuous curves) and with flavor-dependent angular distributions (dotted curves).

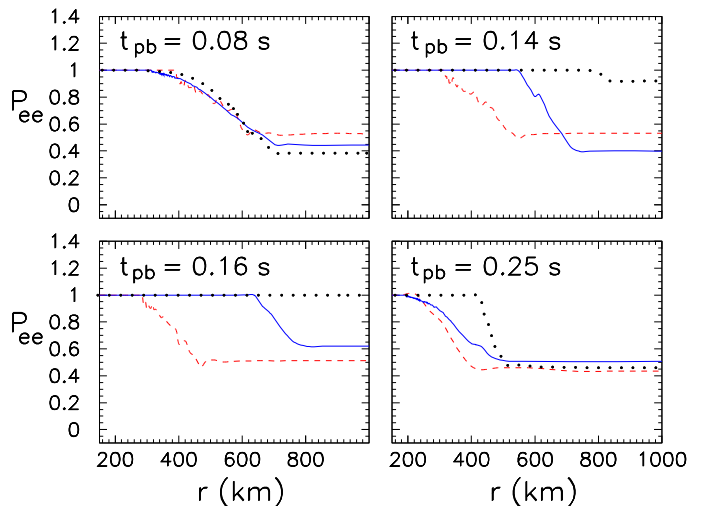


FIG. 6: $8.8 M_{\odot}$ progenitor mass. Radial evolution of the survival probability P_{ee} for electron antineutrinos at different post-bounce times for the MAA evolution with $\lambda = 0$ for a half-isotropic neutrino emission (dashed curves) and in presence of matter effects, with a half-isotropic neutrino emission (continuous curves) and with flavor-dependent angular distributions (dotted curves).

during the accretion phase for two SN models with different progenitor masses. We characterize the SN densities and the neutrino angular spectra with results from recent SN hydrodynamical simulations. We compared the linear stability analysis with the numerical results of the flavor evolution in which we have looked at a local solu-

tion of the equations of motions along a specific line of sight. For the case of an iron-core $10.8 M_{\odot}$ we found that during the accretion phase the dominant matter density strongly suppresses the MAA instability. In particular, including realistic forward-peaked ν angular distributions significantly reduces the strength of the ν - ν interaction term. As a result, in this case the matter suppression of the self-induced flavor conversions would be complete. In the case of a low-mass O-Ne-Mg SN with $8.8 M_{\odot}$ progenitor, where the accretion phase is extremely short, the matter density profile is lower and the ν angular distributions less forward-peaked than in iron-core models. As a consequence, we found that also with realistic angular distributions flavor conversions would be possible at early times, producing in principle interesting time-dependent modulations.

Our analysis is complementary to previous studies [23–25], where some of us explored the matter suppression of self-induced flavor conversions in inverted neutrino mass hierarchy, in axial-symmetric models (see also [26]). The complete suppression of the self-induced effects in both the mass hierarchies for iron-core SNe, implies that the neutrino signal during the accretion phase will be processed only by the ordinary Mikheyev-Smirnov-Wolfenstein effect in the outer stellar layers. This effect would allow in principle to distinguish the neutrino mass hierarchy through the study of the rise time of the SN neutrino signal [33]. The phenomenological importance of our findings motivates further studies with other SN models to confirm the generality of our results. In particular, an accurate characterization of the neutrino angular distributions seems necessary in order to get accurate predictions on the matter suppression. At this regard, in [10] it has been shown that if perfect cylindrical symmetry in the initial neutrino distributions were given up, then super-fast flavor turnovers could occur. These effects cannot be tested within our spherically symmetric SN model. However, recently three-dimensional SN simulations have been carried on, characterizing the neutrino signal during the accretion phase. Surprisingly,

a lepton-emission asymmetry among different flavor has been found [34]. In particular, the electron (anti)neutrino fluxes show a dipole structure, while the ν_x are almost spherically symmetric. We plan to investigate in a future work the role of the matter suppression in this flavor configuration, including also the not axisymmetric neutrino and matter angular distributions.

Self-induced flavor conversions associated with the MAA instability would still be possible for O-Ne-Mg SNe during the accretion phase, and possibly for iron core SNe during the cooling phase, when the matter term becomes sub-dominant with respect to the neutrino-neutrino interaction term. In these situations, a self-consistent treatment of the neutrino equations of motion considering also the flavor evolution along the transverse direction is still lacking. This would imply passing from an ordinary to a partial differential equation problem, adding a big layer of complication in the solution of the equations of motion. This effort is well motivated by the perspective of getting an accurate characterization of the SN neutrino spectral features that would be observable in the planned large underground neutrino detectors [35].

Acknowledgements

We thank T. Fischer, G. Raffelt, S. Sarikas and M. Wu for useful discussions. S.C. acknowledges support from the European Union through a Marie Curie Fellowship, Grant No. PIFI-GA-2011-299861, and through the ITN “Invisibles”, Grant No. PITN-GA-2011-289442. The work of A.M. was supported by the German Science Foundation (DFG) within the Collaborative Research Center 676 “Particles, Strings and the Early Universe.” N.S. acknowledges support from the European Union FP7 ITN INVISIBLES (Marie Curie Actions, PITN-GA-2011-289442). D.S. acknowledges support by the Fundação para a Ciência e Tecnologia (Portugal) under grant SFRH/BD/66264/2009.

-
- [1] J. Pantaleone, “Neutrino oscillations at high densities,” *Phys. Lett. B* **287**, 128 (1992).
 - [2] Y. Z. Qian and G. M. Fuller, “Neutrino-neutrino scattering and matter enhanced neutrino flavor transformation in Supernovae,” *Phys. Rev. D* **51**, 1479 (1995) [astro-ph/9406073].
 - [3] R. F. Sawyer, “Speed-up of neutrino transformations in a supernova environment,” *Phys. Rev. D* **72**, 045003 (2005) [hep-ph/0503013].
 - [4] H. Duan, G. M. Fuller and Y. Z. Qian, “Collective Neutrino Flavor Transformation In Supernovae,” *Phys. Rev. D* **74**, 123004 (2006) [astro-ph/0511275].
 - [5] H. Duan, G. M. Fuller, J. Carlson and Y. Z. Qian, “Simulation of coherent non-linear neutrino flavor transformation in the supernova environment. I: Correlated neutrino trajectories,” *Phys. Rev. D* **74**, 105014 (2006) [astro-ph/0606616].
 - [6] S. Hannestad, G. G. Raffelt, G. Sigl and Y. Y. Y. Wong, “Self-induced conversion in dense neutrino gases: Pendulum in flavour space,” *Phys. Rev. D* **74**, 105010 (2006) [Erratum-ibid. *D* **76**, 029901 (2007)] [astro-ph/0608695].
 - [7] G. L. Fogli, E. Lisi, A. Marrone and A. Mirizzi, “Collective neutrino flavor transitions in supernovae and the role of trajectory averaging,” *JCAP* **0712**, 010 (2007) [arXiv:0707.1998 [hep-ph]].
 - [8] G. L. Fogli, E. Lisi, A. Marrone, A. Mirizzi and I. Tamborra, “Low-energy spectral features of supernova (anti)neutrinos in inverted hierarchy,” *Phys. Rev. D* **78**, 097301 (2008) [arXiv:0808.0807 [hep-ph]].
 - [9] H. Duan, G. M. Fuller and Y. -Z. Qian, “Collective Neutrino Oscillations,” *Ann. Rev. Nucl. Part. Sci.* **60**, 569 (2010) [arXiv:1001.2799 [hep-ph]].

- [10] R. F. Sawyer, “The multi-angle instability in dense neutrino systems,” *Phys. Rev. D* **79** (2009) 105003 [arXiv:0803.4319 [astro-ph]].
- [11] G. G. Raffelt and G. Sigl, “Self-induced decoherence in dense neutrino gases,” *Phys. Rev. D* **75**, 083002 (2007) [hep-ph/0701182].
- [12] A. Esteban-Pretel, S. Pastor, R. Tomàs, G. G. Raffelt and G. Sigl, “Decoherence in supernova neutrino transformations suppressed by deleptonization,” *Phys. Rev. D* **76**, 125018 (2007) [arXiv:0706.2498 [astro-ph]].
- [13] A. Mirizzi and R. Tomàs, “Multi-angle effects in self-induced oscillations for different supernova neutrino fluxes,” *Phys. Rev. D* **84**, 033013 (2011) [arXiv:1012.1339 [hep-ph]].
- [14] A. Banerjee, A. Dighe and G. Raffelt, “Linearized flavor-stability analysis of dense neutrino streams,” *Phys. Rev. D* **84**, 053013 (2011) [arXiv:1107.2308 [hep-ph]].
- [15] G. Raffelt, S. Sarikas and D. d. S. Seixas, “Axial symmetry breaking in self-induced flavor conversion of supernova neutrino fluxes,” *Phys. Rev. Lett.* **111**, 091101 (2013) [arXiv:1305.7140 [hep-ph]].
- [16] S. Samuel, “Bimodal coherence in dense selfinteracting neutrino gases,” *Phys. Rev. D* **53**, 5382 (1996) [hep-ph/9604341].
- [17] G. Raffelt and D. d. S. Seixas, “Neutrino flavor pendulum in both mass hierarchies,” *Phys. Rev. D* **88**, 045031 (2013) [arXiv:1307.7625 [hep-ph]].
- [18] H. Duan, “Flavor Oscillation Modes In Dense Neutrino Media,” *Phys. Rev. D* **88**, 125008 (2013) [arXiv:1309.7377 [hep-ph]].
- [19] A. Mirizzi, “Multi-azimuthal-angle effects in self-induced supernova neutrino flavor conversions without axial symmetry,” *Phys. Rev. D* **88**, 073004 (2013) [arXiv:1308.1402 [hep-ph]].
- [20] A. Mirizzi, “Self-induced spectral splits with multi-azimuthal-angle effects for different supernova neutrino fluxes,” arXiv:1308.5255 [hep-ph].
- [21] G. G. Raffelt and A. Y. Smirnov, “Self-induced spectral splits in supernova neutrino fluxes,” *Phys. Rev. D* **76**, 081301 (2007) [Erratum-ibid. *D* **77**, 029903 (2008)] [arXiv:0705.1830 [hep-ph]].
- [22] A. Esteban-Pretel, A. Mirizzi, S. Pastor, R. Tomas, G. G. Raffelt, P. D. Serpico and G. Sigl, “Role of dense matter in collective supernova neutrino transformations,” *Phys. Rev. D* **78**, 085012 (2008) [arXiv:0807.0659 [astro-ph]].
- [23] S. Chakraborty, T. Fischer, A. Mirizzi, N. Saviano and R. Tomas, “No collective neutrino flavor conversions during the supernova accretion phase,” *Phys. Rev. Lett.* **107**, 151101 (2011) [arXiv:1104.4031 [hep-ph]].
- [24] S. Chakraborty, T. Fischer, A. Mirizzi, N. Saviano and R. Tomas, “Analysis of matter suppression in collective neutrino oscillations during the supernova accretion phase,” *Phys. Rev. D* **84**, 025002 (2011) [arXiv:1105.1130 [hep-ph]].
- [25] N. Saviano, S. Chakraborty, T. Fischer and A. Mirizzi, “Stability analysis of collective neutrino oscillations in the supernova accretion phase with realistic energy and angle distributions,” *Phys. Rev. D* **85**, 113002 (2012) [arXiv:1203.1484 [hep-ph]].
- [26] S. Sarikas, G. G. Raffelt, L. Hudepohl and H. -T. Janka, “Suppression of Self-Induced Flavor Conversion in the Supernova Accretion Phase,” *Phys. Rev. Lett.* **108**, 061101 (2012) [arXiv:1109.3601 [astro-ph.SR]].
- [27] G. Sigl and G. Raffelt, “General kinetic description of relativistic mixed neutrinos,” *Nucl. Phys. B* **406**, 423 (1993).
- [28] L. Wolfenstein, “Neutrino Oscillations In Matter,” *Phys. Rev. D* **17**, 2369 (1978); S. P. Mikheev and A. Yu. Smirnov, “Resonance Enhancement Of Oscillations In Matter And Solar Neutrino Spectroscopy,” *Yad. Fiz.* **42**, 1441 (1985) [*Sov. J. Nucl. Phys.* **42**, 913 (1985)].
- [29] <http://www.nag.com/numeric/fl/manual/html/FLlibrarymanual.asp>
- [30] T. Fischer, S. C. Whitehouse, A. Mezzacappa, F. -K. Thielemann and M. Liebendorfer, “Protoneutron star evolution and the neutrino driven wind in general relativistic neutrino radiation hydrodynamics simulations,” *Astron. Astrophys.* **517** (2010) A80 [arXiv:0908.1871 [astro-ph.HE]].
- [31] J. F. Cherry, J. Carlson, A. Friedland, G. M. Fuller and A. Vlasenko, “Neutrino scattering and flavor transformation in supernovae,” *Phys. Rev. Lett.* **108**, 261104 (2012) [arXiv:1203.1607 [hep-ph]].
- [32] S. Sarikas, I. Tamborra, G. Raffelt, L. Hudepohl and H. -T. Janka, “Supernova neutrino halo and the suppression of self-induced flavor conversion,” *Phys. Rev. D* **85**, 113007 (2012) [arXiv:1204.0971 [hep-ph]].
- [33] P. D. Serpico, S. Chakraborty, T. Fischer, L. Hudepohl, H. -T. Janka and A. Mirizzi, “Probing the neutrino mass hierarchy with the rise time of a supernova burst,” *Phys. Rev. D* **85**, 085031 (2012) [arXiv:1111.4483 [astro-ph.SR]].
- [34] I. Tamborra, F. Hanke, H. -T. Janka, B. Mueller, G. G. Raffelt and A. Marek, “Self-sustained asymmetry of lepton-number emission: A new phenomenon during the supernova shock-accretion phase in three dimensions,” arXiv:1402.5418 [astro-ph.SR].
- [35] S. Choubey, B. Dasgupta, A. Dighe and A. Mirizzi, “Signatures of collective and matter effects on supernova neutrinos at large detectors,” arXiv:1008.0308 [hep-ph].